Thermal conductivity of bulk nanostructured lead telluride in the view of phonon gas kinetics

Takuma Hori[1], Gang Chen[2], and Junichiro Shiomi[1,3,(a)]

[1]*Department of Mechanical Engineering, The University of Tokyo, Hongo Bunkyo-ku, Tokyo, 113-8656, Japan*

[2]*Department of Mechanical Engineering, Massachusetts Institute of Technology, Cambridge, MA 02139, USA*

[3]*Japan Science and Technology Agency, PRESTO, 4-1-8 Honcho, Kawaguchi, Saitama, 332-0012, Japan*

Abstract

Thermal conductivity of lead telluride with embedded nanoinclusions was calculated in the view of phonon-gas Boltzmann transport to understand its potential as thermoelectrics. Using a Monte Carlo method with phonon transport properties obtained from first-principles-based lattice dynamics, simulations of maximum interface-phonon-scattering scenario with the geometrical cross section and volume fraction of the nanoinclusions matched to those of the experiment show that the experiment has already reached the theoretical limit of thermal conductivity. The frequency-dependent analysis further identifies that the thermal conductivity reduction is dominantly attributed to scattering of low frequency phonons and demonstrates mutual adaptability of nanostructuring and local disordering.

(a) Author to whom correspondence should be addressed. Electronic mail: shiomi@photon.t.u-tokyo.ac.jp.

Lead telluride (PbTe) is a promising thermoelectric material for intermediate temperature applications. This is partially attributed to their intrinsically low lattice thermal conductivity (~2 $Wm^{-1}K^{-1}$ at room temperature [1]) since the dimensionless figure of merit, *ZT*, is inversely proportional to the thermal conductivity. Nanostructuring is a growing practical approach to further reduce the lattice thermal conductivity of the bulk materials. A general strategy is to scatter phonons by the nanostructure interfaces without appreciably interfering with the carrier transport. A successful form of bulk nanostructured material has been the sintered nanograins with the nominal grain size smaller and larger than the phonon and carrier mean free paths, respectively [2]. However, the first-principles-based phonon transport calculations of single crystal PbTe indicate that heat is carried mostly by phonons with mean free paths smaller than 10 nm, and the above window of mean free paths does not exist for PbTe [3, 4].

An alternative would be to locally precipitate nanocrystals (nanoinclusions) of different specie inside the PbTe matrix [5-11]. The most successful case to this date is PbTe with strontium telluride (SrTe) nanoinclusions [8, 10], which holds a record ZT = 2.2 at 800 K with appropriate doping and microstructuring. It has been shown that the lattice thermal conductivity can be reduced without sacrificing the electrical conductivity and Seebeck coefficient by achieving the coherent interface between the nanocrystalline precipitates and the matrix ("endotaxial nanostructure").

For further improvement and optimization of the PbTe-based bulk nanostructured thermoelectric materials, it would be helpful to know the theoretical limit of the lattice thermal conductivity. This would give us insights into how well the nanostructured interface is performing to scatter phonons or how further thermal conductivity can be

reduced by optimizing the interface. For the sintered nanograins, the lattice thermal conductivity can be estimated by simplifying the picture with a single grain size value. The first-principles-based anharmonic lattice dynamics calculations [3, 4, 12-14] provide phonon-mean-free-path dependent lattice thermal conductivity, from which thermal conductivity reduction can be calculated for extreme scenarios, e.g. trimming the phonon mean free paths longer than the grain size [15] or enforcing the surface boundary scattering [16]. On the other hand, the effect of nanoinclusions is much less evident since the structure is topologically more complicated.

This work aims to identify a theoretical limit of lattice thermal conductivity of PbTe/nanoinclusion materials in the view of phonon gas kinetics. The simulations of phonon Boltzmann transport under relaxation time approximation were performed for cubic nanoinclusions in a PbTe matrix. By using the frequency/branch dependent phonon transport properties of single crystal PbTe obtained based on first principles, the simulations realize more accurate representation of the intrinsic phonon transport than the simplified empirical models [7, 8, 11]. The maximum interface-scattering scenario is realized by making the PbTe-nanoinclusion interface to completely and diffusively reflect phonons (zero transmission probability).

In the view of phonon gas kinetics, the Boltzmann transport equation of phonon distribution function f under relaxation time approximation is written as

$$\frac{\partial f_s(\omega,\mathbf{r})}{\partial t} + v_s(\omega)\mathbf{e}\cdot\nabla_{\mathbf{r}} f_s(\omega,\mathbf{r}) = -\frac{f_s(\omega,\mathbf{r}) - f_0(\omega,T)}{\tau_s(\omega,T)} \tag{1}$$

where s, ω, $\mathbf{r}$, v, f_0 , T, and τ are, phonon polarization, frequency, position, group velocity, Bose Einstein distribution, temperature, and relaxation time, respectively. In this study, to realize the calculation of the nanostructured geometry, Boltzmann transport equation was stochastically solved by Monte Carlo method [17-22]. Here, only

the longitudinal acoustic (LA) and transverse acoustic (TA) branches are considered since the contributions of optical modes to PbTe lattice thermal conductivity are much smaller than those of acoustic modes [3]. The energy-based variance-reduced Monte Carlo formulations[21] with the effective energy of the phonon particle $\varepsilon = 8.6 \times 10^{-26}$J were applied to ensure the accuracy and speed of the simulations.

The geometry of a typical simulation cell is shown in Fig. 1, where a cubic nanoinclusion is arranged in the middle of the simulation cell. With the aim to model the maximum interface-scattering scenario, PbTe-nanoinclusion interfaces were modeled to give the largest thermal resistance. This was done by setting the phonon transmission probability across the interface to zero i.e. applying the total diffusive reflection condition with the Lambert's cosine law. Therefore, the nanoinclusion is essentially a nanovoid, in which phonon transport does not need to be considered. This does not only make the simulation simple but also exclude uncertainties in modeling the interface and thus in identifying the theoretical limit of lattice thermal conductivity for a given nanoinclusion size and volume fraction. Here, we do not account for the anisotropy in the reflection direction due to the wave scattering characteristics[23]. However, we have confirmed that altering the reflection from diffusive to specular does not reduce the thermal conductivity. The length of the nanoinclusion a is varied from 1 nm to 20 nm. For each a, the dependence of the lattice thermal conductivity on the nanoinclusion volume fraction was studied by varying L. The scattering cross section here is the geometrical one, and, for simplicity, we do not consider the wave-vector dependent variation of the cross section due to the wave scattering[24].

The simulation models the steady heat conduction through 3-d periodic nanostructures in an infinite domain. For this, the periodic boundary condition is

applied in the y and z directions, and the *periodic distortion boundary condition* [20, 21] in the x direction (direction of heat flow). The periodic distortion boundary condition imposes periodicity only to the distortions of the distribution functions (f-f_0), which enables us to prescribe different temperatures to the left and right virtual boundary through f_0 [20, 21]. With the boundary conditions, the simulation of a unitary cell allows us to access properties of steady state heat conduction through a periodic structure (Fig. 1).

The simulation is initialized by randomly placing phonons in the simulation cell with frequency and polarization distributions determined by the density of states and Bose Einstein statistics. Each phonon is initially given a random propagation direction. The simulation cell is divided into subcells to define the local temperatures calculated from their phonon energy. After the initialization, each phonon propagates in certain direction at its group velocity. The phonon group velocity and density of states of a single crystal PbTe were calculated in advance using the harmonic interatomic force constants obtained from first principles. The group velocity calculated over the first Brillouin zone was averaged for each branch to be a function of frequency (Fig. 2).

Within each time step Δt, a phonon may be scattered by other phonons (intrinsic phonon-phonon scattering) or at the interface. The intrinsic phonon scattering occurs with the probability P=1-exp(-$\Delta t/\tau$) and resets all the phonon states (frequency, polarization, and propagation direction). The frequency- and temperature-dependent relaxation time of the single crystal PbTe was calculated in advance by Fermi's golden rule of three-phonon scattering processes, using the anharmonic interatomic force constants obtained based on first principles calculations [3]. The results with finite wavevector-space mesh were fitted by the Klemens expression $C\omega^{-2}$, where C is a

constant (Fig. 2). The obtains values are C=2.89×10^{14} s^{-1} and 1.44×10^{14} s^{-1} at 300 K and 600 K, respectively.

The simulations are performed for two different average temperatures 300 K and 600 K. The time step of the simulation is 0.05 ps for both temperatures. The temperature difference between hot and cold boundaries is set to be ΔT=0.2 K. The convergence to a steady heat flux with a linear temperature gradient is achieved in 200,000 time steps, and then data were sampled for another 200,000 time steps to calculate the lattice thermal conductivity. The lattice thermal conductivity is calculated from the Fourier's law, $\kappa_{lat} = qL/\Delta T$, where q and L are the heat flux and the length of the simulation cell in the x direction, respectively. The heat flux is calculated as $q = \sum \varepsilon l_x / V$, where $\varepsilon$and l_x are the phonon energy and start-to-end distance in a unit time. The lattice thermal conductivity was time-averaged to reduce the statistical noise in the heat flux. For each nanoinclusion size and volume fraction, 6 different simulations were conducted and ensemble-averaged to further enhance the signal to noise ratio.

In Fig. 3, the calculated lattice thermal conductivity is plotted with respect to the volume fraction of the nanoinclusion a^3/L^3. This identifies the minimum thermal conductivity for a given geometrical cross section and volume fraction of the cubic nanoinclusions. For 1 nm nanoinclusions with a realistic volume fraction, thermal conductivity was reduced by about 60 %, and the reduction ratio decreases with the temperature. Although here we only show the data for a unit cell with one nanoinclusion, we have also performed simulations of more random configurations with multiple nanoinclusions per unit cell, which, for the same nanoinclusion size and volume fraction, resulted in no thermal conductivity difference as has been already found in the previous

study [19].

At 300 K, the calculated lattice thermal conductivity in the cases of a=1 nm and 2 nm agrees well with the experiments of PbTe with SrTe nanoinclusions with the corresponding average size [8]. The agreement indicates that the lattice thermal conductivity in the experiment has reached the theoretical limit of thermal conductivity in view of the phonon gas kinetics. One could argue that some strains, dislocations, and impurities should be present in the PbTe matrix in the experiment and they could also contribute to the reduction of the lattice thermal conductivity while the calculation thus far assumes a pure PbTe crystal. However, adding these effects would result in weaker volume fraction dependence, and thus enlarge the discrepancy between the calculation and experiment. Therefore, the agreement in the volume fraction dependence at 300 K suggests validity to assume the pure impurity/defect free PbTe matrix. It should be noted that there still remains uncertainty in the comparison as the lattice thermal conductivity in the experiment at 600 K decreases more sharply with increasing volume fraction than in the calculations. Nevertheless, the current calculation results suggest that the nanostructure interface in the experiments is extremely effective in resisting the phonon transport. This may seem counterintuitive since the PbTe-nanoinclusion interfaces in the experiment was observed to be coherent, however, the coherence could also cause strong residual strain and stress, which may serve as an effective scatterer of phonons.

Figure 4 shows the dependence of the lattice thermal conductivity on the nanoinclusion size (a) at room temperature. For all the volume fractions, the dependence becomes stronger as a decreases, and one-nanometer variation in a could significantly influence the extent of thermal conductivity reduction when a is smaller

than 10 nm, which is consistent with the mean free path distribution of phonon with noticeable contribution to heat conduction[3]. This indicates the importance of making the nanoinclusion size down to 1~2 nm as was done in the experiments [8]. The thermal conductivity could be further reduced by making *a* even smaller than 1 nm, but one needs to be careful with the limit of the current particle collision picture when *a* becomes smaller than the phonon wave packet size. The calculations of the wave characteristics are underway but are not the scope of this work.

The current simulation also helps us study the microscopic picture of lattice thermal conductivity reduction by the nanoinclusions. To this end, we introduce the frequency dependent lattice thermal conductivity and compare the single crystal and nanostructured material (3.7 %, a = 1 nm) at 300 K. Figure 5 shows that the lattice thermal conductivity reduction by the nanoinclusions mostly occurs for the low frequency phonons. The high frequency phonons (over 8 THz) are weakly affected because the mean free paths of those phonons are shorter than the nanoinclusion length.

The above frequency analysis suggests that the nanostructuring can be well combined with introducing local disorders (e.g. point defects and impurities), whose phonon scattering rate, in analogy to the Rayleigh scattering, can be roughly approximated to scale with $\sim\omega^4$. This is implemented in the Monte Carlo simulations through the relaxation time τ using the Matthiessen's rule as, $\tau^{-1} = \tau_{\text{int}}^{-1} + B\omega^4$, where τ_{int} and B are the intrinsic relaxation time of PbTe and an empirical constant, respectively. The result shown in Fig. 5 was calculated for $B = 1.0 \times 10^{-40}$ s^3, a value that gives the same extent of lattice thermal conductivity reduction as in PbTe/PbSe solid solution in the experiments (40 %) [25].

Figure 5 plots the frequency-dependent lattice thermal conductivity by the

local-disorder scattering. The figure shows that the presence of the local disorders nearly diminishes the thermal conductivity of phonons with frequency higher than 8 Hz without sacrificing the reduction in low frequency caused by nanoinclusions. This results in a large thermal conductivity reduction in the entire frequency regime, demonstrating the mutual adaptability of nanostructuring and local disordering. As seen in Fig. 5, the combined approach can reduce the total PbTe lattice thermal conductivity by about 75 % with 3.7% nanoinclusions, which is significantly more than the reduction caused solely by nanoinclusions (60 %) or by local disorders (40 %).

In summary, we have performed the Monte Carlo simulations of Boltzmann phonon transport in PbTe with embedded cubic nanoinclusions using the accurate bulk phonon transport properties obtained from first-principles-based lattice dynamics. The simulations under the maximum interface-phonon-scattering scenario identify the lower-limit lattice thermal conductivity of the nanostructured material in the view of phonon-gas Boltzmann transport. The results suggest that the nanostructure interface in the previous experiments is extremely effective in resisting the phonon transport. The frequency dependent analysis further identified that the resistance is mainly attributed to scattering of low frequency phonons by the nanoinclusions. This suggests the mutual adaptability with local disordering whose scattering rates increases with phonon frequency. A test case with a realistic alloy concentration shows that the combined approach can significantly reduce thermal conductivity.

ACKNOWLEDGEMENT

This work is partially supported by Research Fellow ships of the Japan Society for the Promotion of Science for Young Scientists, Japan Science and Technology Agency,

PRESTO, KAKENHI 23760178, the Thermal & Electric Energy Technology Foundation (TH and JS), and by the “Solid State Solar-Thermal Energy Conversion Center (S3TEC),” an Energy Frontier Research Center funded by the U.S. Department of Energy, Office of Science, Office of Basic Energy Sciences under Grant No. DE-SC0001299/DE-FG02-09ER46577 (GC).

References

[1] I.U.I. Ravich, B.A. Efimova, I.A. Smirnov, Semiconducting lead chalcogenides, Plenum Press, New York,, 1970.

[2] B. Poudel, Q. Hao, Y. Ma, Y. Lan, A. Minnich, B. Yu, X. Yan, D. Wang, A. Muto, D. Vashaee, X. Chen, J. Liu, M.S. Dresselhaus, G. Chen, Z. Ren, High-thermoelectric performance of nanostructured bismuth antimony telluride bulk alloys, Science, 320(5876) (2008) 634-638.

[3] T. Shiga, J. Shiomi, J. Ma, O. Delaire, T. Radzynski, A. Lusakowski, K. Esfarjani, G. Chen, Microscopic mechanism of low thermal conductivity in lead telluride, Physical Review B, 85(15) (2012) 155203.

[4] Z. Tian, J. Garg, K. Esfarjani, T. Shiga, J. Shiomi, G. Chen, Phonon conduction in PbSe, PbTe, and PbTe_{1−x}Se_{x} from first-principles calculations, Physical Review B, 85(18) (2012) 184303.

[5] K.F. Hsu, S. Loo, F. Guo, W. Chen, J.S. Dyck, C. Uher, T. Hogan, E.K. Polychroniadis, M.G. Kanatzidis, Cubic AgPbmSbTe2+m: Bulk thermoelectric materials with high figure of merit, Science, 303(5659) (2004) 818-821.

[6] M.G. Kanatzidis, Nanostructured Thermoelectrics: The New Paradigm?, Chem Mater, 22(3) (2010) 648-659.

[7] J.Q. He, S.N. Girard, M.G. Kanatzidis, V.P. Dravid, Microstructure-Lattice Thermal Conductivity Correlation in Nanostructured PbTe0.7S0.3 Thermoelectric Materials, Advanced Functional Materials, 20(5) (2010) 764-772.

[8] K. Biswas, J.Q. He, Q.C. Zhang, G.Y. Wang, C. Uher, V.P. Dravid, M.G. Kanatzidis, Strained endotaxial nanostructures with high thermoelectric figure of merit, Nat Chem, 3(2) (2011) 160-166.

[9] Y.Z. Pei, J. Lensch-Falk, E.S. Toberer, D.L. Medlin, G.J. Snyder, High Thermoelectric Performance in PbTe Due to Large Nanoscale Ag-2 Te Precipitates and La Doping, Advanced Functional Materials, 21(2) (2011) 241-249.

[10] K. Biswas, J. He, I.D. Blum, C.I. Wu, T.P. Hogan, D.N. Seidman, V.P. Dravid, M.G. Kanatzidis, High-performance bulk thermoelectrics with all-scale hierarchical architectures, Nature, 489(7416) (2012) 414-418.

[11] S.-H. Lo, J. He, K. Biswas, M.G. Kanatzidis, V.P. Dravid, Phonon Scattering and Thermal Conductivity in p-Type Nanostructured PbTe-BaTe Bulk Thermoelectric Materials, Advanced Functional Materials, 22(24) (2012) 5175-5184.

[12] K. Esfarjani, H.T. Stokes, Method to extract anharmonic force constants from first principles calculations, Physical Review B, 77(14) (2008) 144112.

[13] K. Esfarjani, G. Chen, H.T. Stokes, Heat transport in silicon from first-principles calculations, Physical Review B, 84(8) (2011) 085204.
[14] J. Shiomi, K. Esfarjani, G. Chen, Thermal conductivity of half-Heusler compounds from first-principles calculations, Physical Review B, 84(10) (2011) 104302.
[15] A.J. Minnich, J.A. Johnson, A.J. Schmidt, K. Esfarjani, M.S. Dresselhaus, K.A. Nelson, G. Chen, Thermal Conductivity Spectroscopy Technique to Measure Phonon Mean Free Paths, Physical Review Letters, 107(9) (2011) 095901.
[16] F. Yang, C. Dames, Mean free path spectra as a tool to understand thermal conductivity in bulk and nanostructures, Physical Review B, 87(3) (2013) 035437.
[17] S. Mazumder, A. Majumdar, Monte Carlo Study of Phonon Transport in Solid Thin Films Including Dispersion and Polarization, Journal of Heat Transfer, 123(4) (2001) 749.
[18] D. Lacroix, K. Joulain, D. Lemonnier, Monte Carlo transient phonon transport in silicon and germanium at nanoscales, Physical Review B, 72(6) (2005) 064305.
[19] M.-S. Jeng, R. Yang, D. Song, G. Chen, Modeling the Thermal Conductivity and Phonon Transport in Nanoparticle Composites Using Monte Carlo Simulation, Journal of Heat Transfer, 130(4) (2008) 042410.
[20] Q. Hao, G. Chen, M.-S. Jeng, Frequency-dependent Monte Carlo simulations of phonon transport in two-dimensional porous silicon with aligned pores, Journal of Applied Physics, 106(11) (2009) 114321.
[21] J.-P.M. Péraud, N.G. Hadjiconstantinou, Efficient simulation of multidimensional phonon transport using energy-based variance-reduced Monte Carlo formulations, Physical Review B, 84(20) (2011) 205331.
[22] A. Jain, Y.-J. Yu, A.J.H. McGaughey, Phonon transport in periodic silicon nanoporous films with feature sizes greater than 100 nm, Physical Review B, 87(19) (2013) 195301.
[23] N. Zuckerman, J.R. Lukes, Acoustic phonon scattering from particles embedded in an anisotropic medium: A molecular dynamics study, Physical Review B, 77(9) (2008) 094302.
[24] W. Kim, A. Majumdar, Phonon scattering cross section of polydispersed spherical nanoparticles, Journal of Applied Physics, 99(8) (2006).
[25] H. Wang, A.D. LaLonde, Y.Z. Pei, G.J. Snyder, The Criteria for Beneficial Disorder in Thermoelectric Solid Solutions, Advanced Functional Materials, 23(12) (2013) 1586-1596.

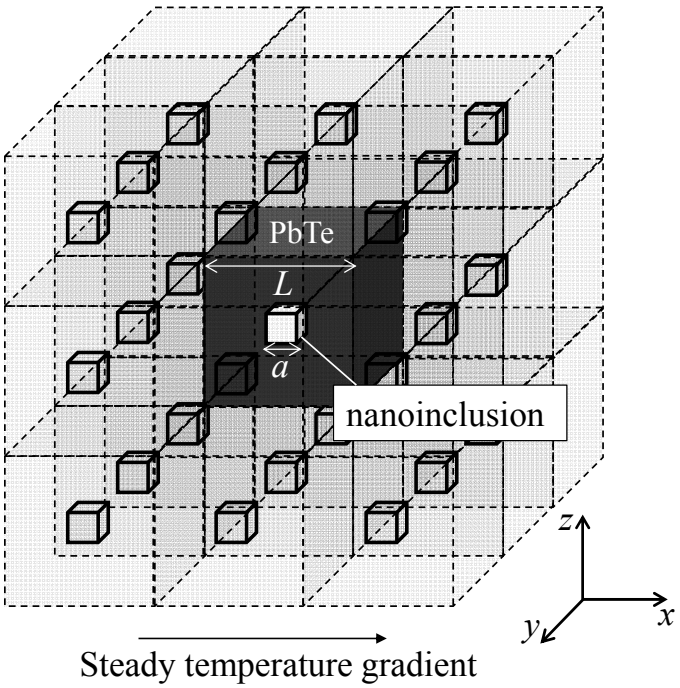

Figure 1. A schematic of the Monte Carlo simulation cell of phonon transport in PbTe with nanoinclusions. The nanoinclusion is arranged at the center of the simulation cell. The periodic distortion boundary condition [20] is applied in the *x* direction and the periodic boundary condition in the *y*-*z* plane.

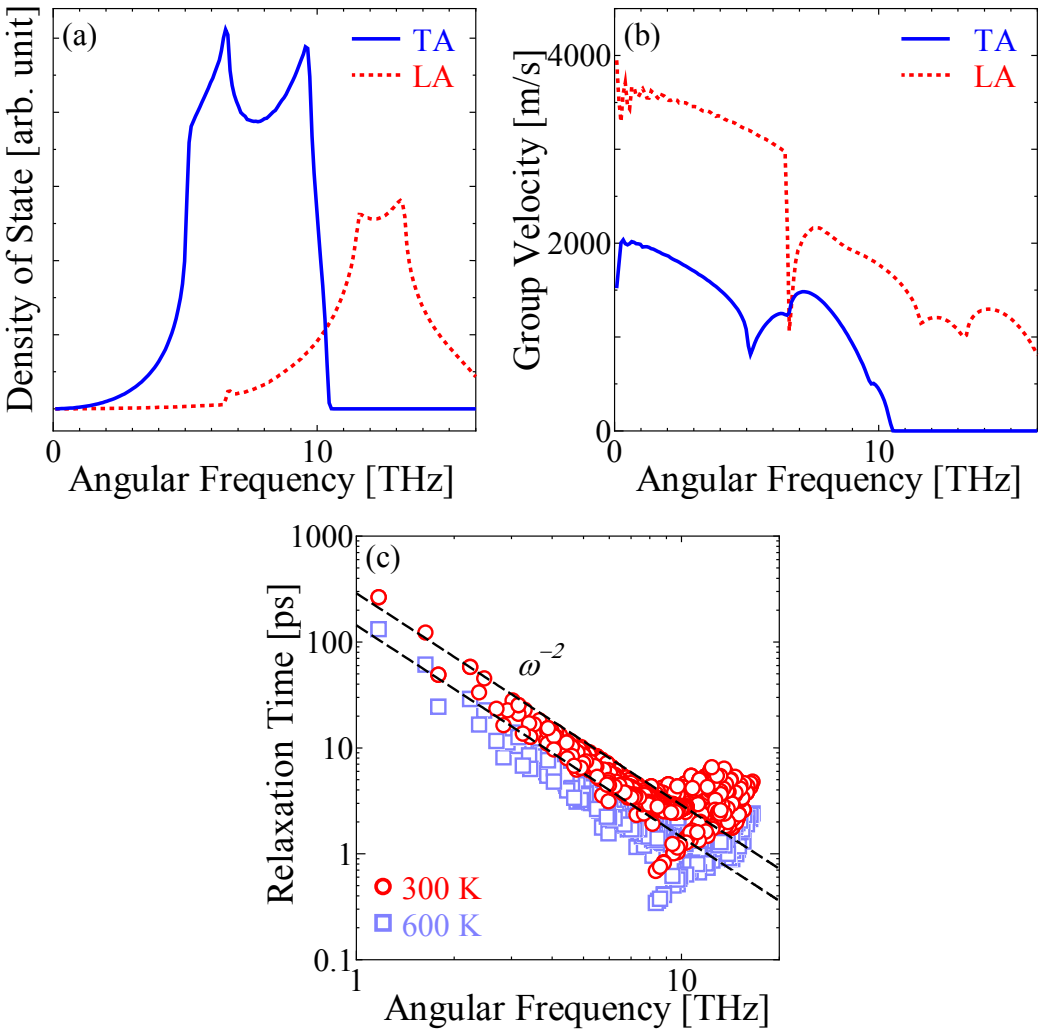

Figure 2. The frequency- and branch-dependent phonon transport properties, (a) the density of states, (b) group velocity, and (c) relaxation time, obtained from the first-principles based anharmonic lattice dynamics calculations. TA and LA denote the transverse and longitudinal acoustic branches.

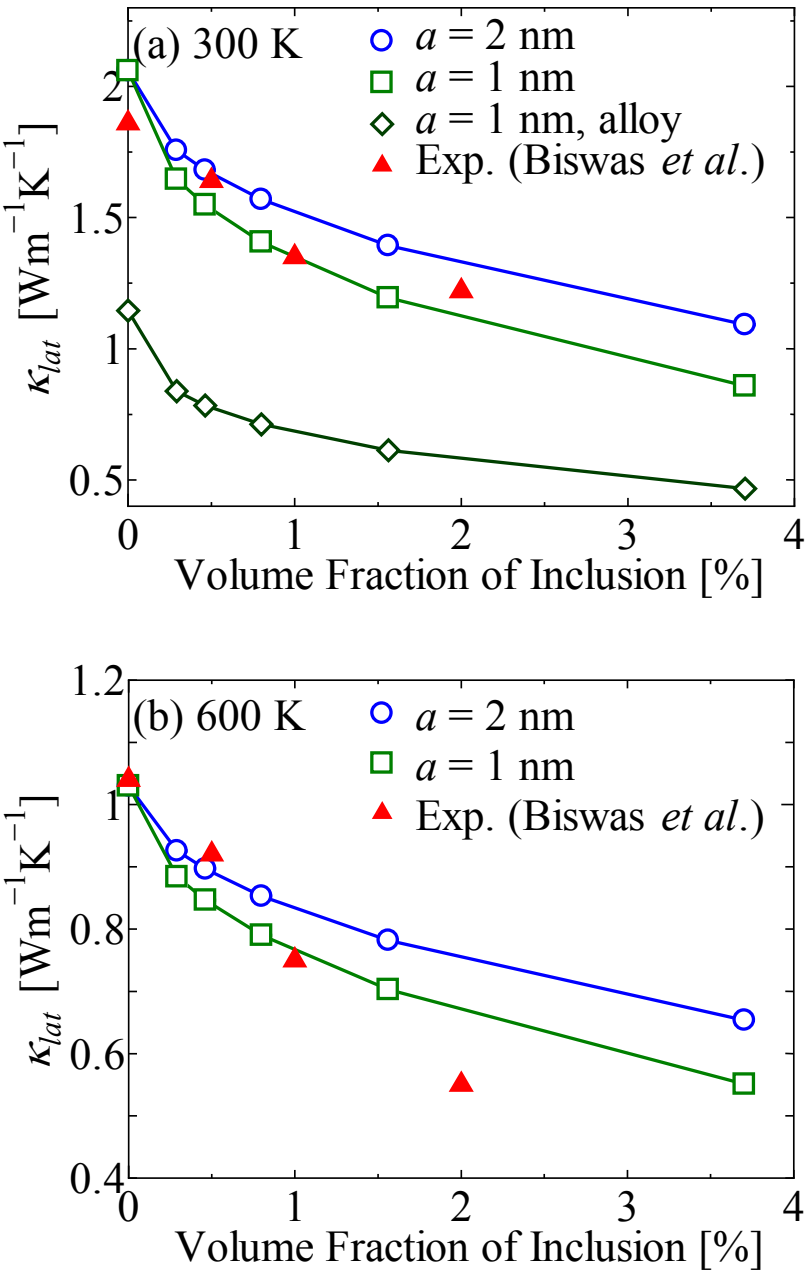

Figure 3. Nanoinclusion volume-fraction dependence of lattice thermal conductivity κ_{lat} of the PbTe nanocomposites at (a) 300 K and (b) 600 K. The length of the nanoinclusion a is set to 1 or 2 nm. The results are compared with the experiments of PbTe/SrTe coherent ("endotaxial") nanocomposites [8].

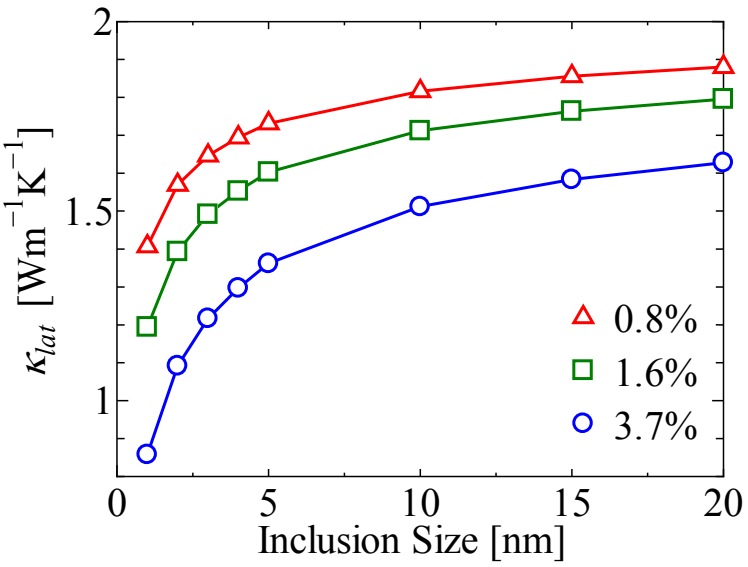

Figure 4. Nanoinclusion size dependence of the lattice thermal conductivity κ_{lat} of the PbTe nanocomposites at 300 K for volume fractions 0.8, 1.6, and 3.7 %.

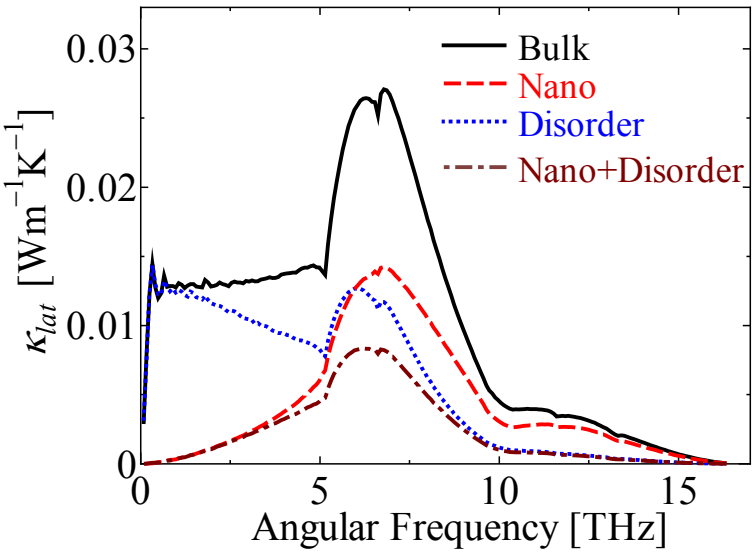

Figure 5. Frequency dependence of lattice thermal conductivity κ_{lat} of PbTe nanocomposite at 300 K. The legends "Nano" and "disorder" indicate the PbTe with nanoinclusions (3.7 %, a = 1 nm) and local disorders ($B = 1.0 \times 10^{-40}$ s^3), respectively.

Supporting information

Lower-limit thermal conductivity of bulk nanostructured lead telluride in the view of phonon gas kinetics

Takuma Hori, Gang Chen, and Junichiro Shiomi

Prior to calculations of PbTe with the nanoinclusions, Monte Carlo simulations were performed to obtain the lattice thermal conductivity of bulk single crystal PbTe. The simulations were performed for two different averaged temperatures 300 K and 600 K. The length of the cubic simulation L was varied from 3 to 14 nm to investigate the length dependence in the simulations. The simulation method and parameters are the same as the cases with nanoinclusion except that there is no interface in this case. The results of the simulations are shown in Fig. S1. The calculated lattice thermal conductivity was 2.05 $Wm^{-1}K^{-1}$ and 1.03 $Wm^{-1}K^{-1}$ with uncertainty of around 0.1 % at 300 K and 600 K, respectively. These values were compared with the analytical solution of the phonon Boltzmann transport equation [Eq. (1)],

$$\kappa_{lat} = \frac{1}{3}\sum_{s}\int D_s \hbar\omega \frac{\partial f_0}{\partial T} v_s^{\,2} \tau_s d\omega , \tag{S1}$$

where D is the phonon density of states. By substituting the phonon transport properties of bulk PbTe, the lattice thermal conductivity was obtained to be 2.06 $Wm^{-1}K^{-1}$ and 1.03 $Wm^{-1}K^{-1}$ at 300 K and 600 K, respectively. The good agreement between the Monte Carlo simulations and the Boltzmann transport equation indicates that the simulations in this study can correctly reproduce the kinetics of phonons. In addition, as seen in the figure, the calculated lattice thermal conductivity at both temperatures shows only negligible dependence on L, confirming the validity in adopting the simulation cell as

small as 3 nm.

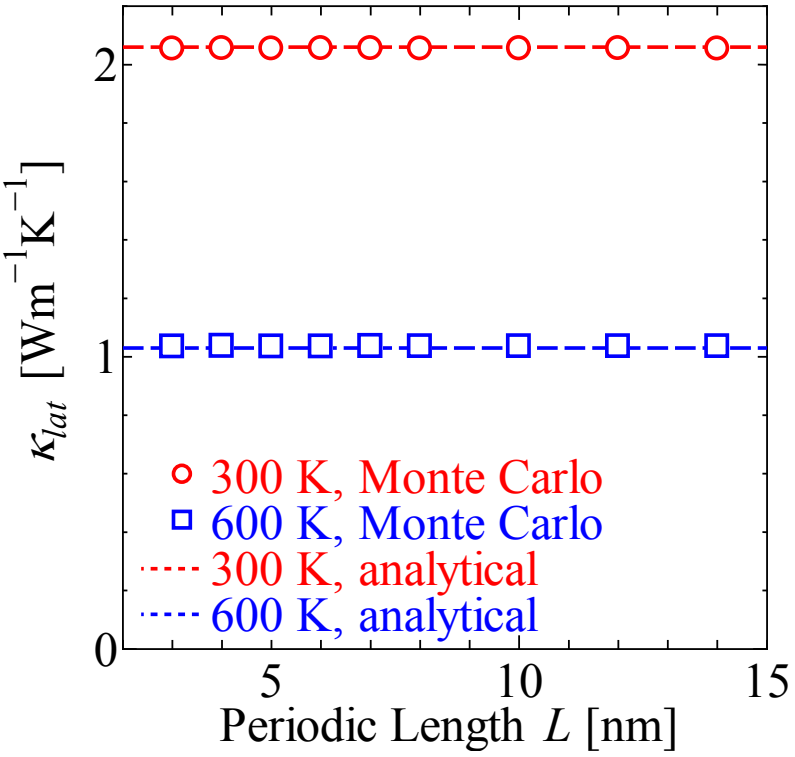

Figure S1. Periodic length L dependence of lattice thermal conductivity κ_{lat} of PbTe at 300 K and 600 K calculated by Monte Carlo simulations. The analytical solutions were calculated from Eq. [1].